International Journal of Mechanical Sciences 50 (2008) 1344–1353

Contents lists available at ScienceDirect

International Journal of Mechanical Sciences

journal homepage: www.elsevier.com/locate/ijmecsci

Effect of small harmonic oscillations during the steady rolling of a cylinder on a plane

J.R. Barber [a,*], M. Ciavarella [b], L. Afferrante [b], A. Sackfield [c]

[a] Department of Mechanical Engineering, University of Michigan, Ann Arbor, MI 48109-2125, USA
[b] CEMEC-PoliBA - Centre of Excellence in Computational Mechanics, V.le Japigia 182, Politecnico di Bari, 70125 Bari, Italy
[c] Department of Mathematics, Statistics and Operational Research, Nottingham Trent University, Nottingham, NG1 4BU, UK

ARTICLE INFO

Article history:
Received 31 January 2008
Accepted 31 July 2008
Available online 3 August 2008

Keywords:
Rolling contact
Rail corrugations
Contact mechanics
Microslip

ABSTRACT

If a wheel rolling over a rail transmits a tangential traction, frictional microslip occurs in part of the contact area, resulting in energy dissipation and localized wear. If the applied forces oscillate in time, the resulting wear will be non-uniform, resulting in 'corrugations' that can grow with progressive passes, depending on the dynamics of the overall system. In this paper, a linear perturbation method is used to obtain closed-form expressions for the receptance of a two-dimensional rolling contact subjected to small oscillations in normal force and rotational speed superposed on a mean value in the limit of large coefficient of friction. Corresponding expressions are also obtained for the amplitude and phase of the energy dissipation in the contact, which is expected to correlate with the local wear rate.

The results are compared with a simpler Winkler model of the contact and with other models that have been used for the analysis of rail corrugation. Surprisingly good agreement is obtained with numerical results due to Gross-Thebing for the receptances due to oscillations in rotational speed.

1. Introduction

Railway tracks have a tendency to develop periodic perturbations known as 'corrugations' which cause undesirable noise and possible lack of traction. Corrugation has been a subject of experimental and theoretical study for 80 years and numerous explanations have been advanced. It is generally agreed that the phenomenon results from an unstable interaction between the dynamics of the moving vehicle, the dynamics of the track and the wear mechanism at the wheel/rail contact, but these are all complex processes and authors disagree as to the relative importance of the many contributing factors.

Theoretical models broadly speaking fall into two categories. Some authors use a fully numerical treatment and endeavour to include the most accurate possible description of all features of the problem. Such models can be explored to determine the effect of system and operating parameters, but it is difficult to draw conclusions of any generality or to pinpoint the reasons for any discrepancy between predictions and experimental observations. Other authors deliberately idealize the system, including only those features which they regard as important in determining the qualitative behaviour in the hope that the resulting relative simplicity will enable the effects of different aspects of the system to be more clearly delineated. Of course, in this case everything depends on whether the idealized model adequately described the more important physical mechanisms.

Arguably the most challenging element to represent by a theoretical model is the mechanics of rolling contact between the wheel and the rail. Archard's wear law [1] suggests that rail wear will occur in regions where there is frictional microslip and that the wear rate will be proportional to the rate of frictional energy dissipation per unit area. Carter [2] solved the problem of steady rolling of a cylinder on a plane with traction or braking and identified the extent of the microslip region at the trailing edge and the resulting traction distribution. Various approximate and numerical methods have been used to extend his result to more realistic three-dimensional rail wheel contacts [3, Section 8.4]. However, for corrugations to form it is necessary that the wear rate should vary in time and space and hence a transient solution of the contact problem is necessary.

A simple approximation used by many authors is to perform a perturbation analysis on the steady-state relation between wear rate, creep velocity and normal force. This implies that the steady-state relation is equally applicable under transient conditions, which is plausible if conditions change relatively slowly. Kalker [4,5] has obtained analytical and numerical solutions of several two-dimensional transient rolling contact problems and his results show that the 'memory' of the system is more or less restricted to the time it takes for a point to transit from the leading edge to the trailing edge of the contact region. Thus, if the

* Corresponding author.
E-mail address: jbarber@umich.edu (J.R. Barber).

0020-7403/$ - see front matter © 2008 Elsevier Ltd. All rights reserved.
doi:10.1016/j.ijmecsci.2008.07.011

contact region has a mean semi-width a_0 in the direction of rolling it is reasonable to assume that the steady-state solution will adequately describe the transient behaviour if the wavelength λ of the corrugation satisfies the condition $\lambda \gg 2a_0$. Alternatively, if we define a temporal frequency ω for the resulting vibration, the steady-state approximation is reasonable if

$$\zeta \equiv \frac{2\omega a_0}{V} = \frac{4\pi a_0}{\lambda} \ll 1, \tag{1}$$

where V is the vehicle speed. For railway applications, typical contact semi-widths lie in the range 3–5 mm and the shortest corrugation wavelengths of interest are about 20 mm, giving a range $0 < \zeta < 5$.

For large values of ζ, the rolling velocity is slow compared with the oscillation due to corrugations and we would expect the response to the latter to be similar in form to that described by Mindlin and Deresiewicz [6] for a static contact subject to oscillatory loads. In this case, the contact can be represented by a spring and a hysteretic damper and several authors have therefore developed modified contact models by adding additional spring and damping terms to the perturbed steady state solution [7].

An alternative approach is to replace the exact elasticity solution of the contact problem by a 'Winkler' approximation[1] in which the surface displacements of the contacting bodies are proportional only to the *local* tractions [8]. In particular this is the basis of the 'simplified' theory of Kalker [9] and of his numerical algorithm 'FASTSIM' [10]. The constants of proportionality (the normal and tangential moduli of the foundation) can be chosen so as to make some of the predictions of the simplified theory agree with the exact results for one particular loading. For example, in the two-dimensional rolling problem they can be tuned to the perturbed Carter solution, in which case some of the predictions will be exact in the limit $\zeta \to 0$ [11]. However, we would expect the accuracy of the simplified theory to deteriorate as we move further from this reference condition and there is no way to estimate even the qualitative nature of this deviation.

In the present paper, we shall explore this issue by developing an elasticity solution for the two-dimensional problem of a rolling cylinder where the applied loads comprise a mean value with a small superposed sinusoidal oscillation. In particular, we shall obtain the frequency-dependent receptances defining the relations between the amplitudes of the oscillating forces and the corresponding relative displacements in the limit of large coefficient of friction. We shall also obtain the corresponding expressions for frictional energy dissipation which, in view of the wear law, can be used to determine whether a given corrugation would be stable or unstable when combined with a suitable model of the rest of the dynamic system.

2. Problem statement

Suppose that the vehicle is moving to the left at constant speed V, so that the wheel is rotating counter-clockwise at some speed $\Omega(t)$, where t is time. We superpose a rigid-body velocity V to the right, bringing the center of the wheel to rest and causing the rail to move at speed V to the right. We assume that the vehicle is braking, so that the braking torque T_B opposes the direction of rotation and the friction force Q on the wheel opposes the motion V, as shown in Fig. 1. However, the corresponding case of an accelerating vehicle can be shown to lead to identical expressions for the receptances. The normal contact force (compressive positive) is denoted by P. Since we are considering

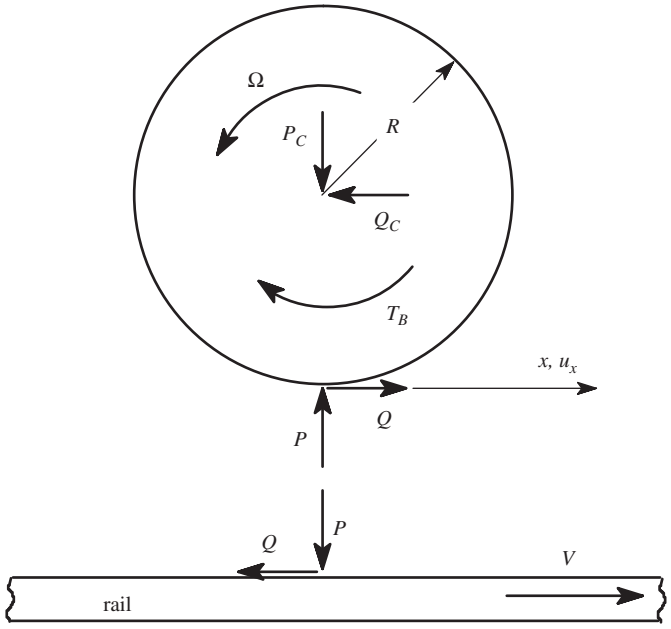

Fig. 1. System geometry.

the transient problem, the wheel will experience translational and rotational accelerations, so the forces P_C, Q_C at the axle will not generally be equal and opposite to P, Q. Fig. 1 also shows the sign convention for the coordinate x and for the elastic displacement u_x of a point on the wheel in the contact zone.

If there were no elastic deformation, the velocity of a point on the wheel in the contact region in the x-direction would be $\Omega(t)R$. However, the steady-state tensile strain $\partial u_x/\partial x$ increases the circumference of the wheel and hence increases this velocity in the proportion $(1 + \partial u_x/\partial x)$. Also, if the elastic displacement varies in time, we have an additional elastic velocity $\partial u_x/\partial t$. Adding these contributions, the rightward velocity of a point on the wheel is

$$v_x = \left(1 + \frac{\partial u_x}{\partial x}\right)\Omega(t)R + \frac{\partial u_x}{\partial t} = \Omega(t)R + V\frac{\partial u_x}{\partial x} + \frac{\partial u_x}{\partial t},$$

where we have replaced $\Omega(t)R$ by V in the second term since the difference is second order.

We choose to concentrate all the elastic deformation in the wheel, which means that we shall use an equivalent modulus for the wheel and treat the rail as rigid. In that case, points on the rail move at constant speed V to the right and it follows that in regions where there is no slip, $v_x = V$ and hence

$$V\frac{\partial u_x}{\partial x} + \frac{\partial u_x}{\partial t} = V - \Omega(t)R. \tag{2}$$

We consider the case where a small sinusoidal perturbation is superposed on the steady state and hence $u_x(x,t), \Omega(t)$ can be written

$$u_x(x,t) = u_0(x) + u_1(x)\exp(\imath\omega t), \quad \Omega(t) = \Omega_0 + \Omega_1\exp(\imath\omega t). \tag{3}$$

In this and subsequent expressions containing complex exponential factors, it is implied that the real part is taken in determining the physical quantities $u_x(x,t), \Omega(t)$. Substituting these results into Eq. (2), separating out the exponential terms and solving the resulting ordinary differential equations in x, we obtain

$$u_0(x) = \left(1 - \frac{\Omega_0 R}{V}\right)x + C_0, \quad u_1(x) = \frac{\imath\Omega_1 R}{\omega} + C_1\exp\left(-\frac{\imath\omega x}{V}\right), \tag{4}$$

where C_0, C_1 are arbitrary constants to be determined from the boundary conditions.

[1] This is sometimes referred to as the 'wire brush' model.

3. The contact problem

We assume that both the normal and tangential forces P, Q have the sinusoidal form

$$P(t) = P_0 + P_1 \exp(\imath\omega t), \quad Q(t) = Q_0 + Q_1 \exp(\imath\omega t), \tag{5}$$

where P_0, P_1, Q_0, Q_1 are constants and $P_1 \ll P_0$, $Q_1 \ll Q_0$.

The instantaneous contact semi-width a is related to P through the Hertzian equation [3],

$$a = \sqrt{\frac{4PR}{\pi E^*}}, \tag{6}$$

where E^* is the plane strain composite elastic modulus. Since the perturbation is small, we can write

$$a(t) = a_0 + a_1 \exp(\imath\omega t), \tag{7}$$

where

$$a_0 = \sqrt{\frac{4P_0R}{\pi E^*}} \quad \text{and} \quad a_1 = P_1 \frac{\partial a}{\partial P} = P_1 \sqrt{\frac{R}{P_0 \pi E^*}} = \frac{P_1 a_0}{2P_0}. \tag{8}$$

For finite values of the coefficient of friction, the contact area would comprise a stick zone $-a(t) < x < l(t)$ adjacent to the leading edge and a microslip zone $l(t) < x < a(t)$ at the trailing edge, as in Carter's steady-state solution. However, if the coefficient of friction is sufficiently large, the slip zone becomes negligibly small and the contact problem can be solved under conditions of full stick. In this limit, the contact tractions must be bounded at the leading edge and will generally be square-root singular at the trailing edge. In fact, the strength of this singularity, analogous to a mode II stress intensity factor, is a measure of the energy dissipated in friction in the vanishingly small slip zone and will be calculated as part of the solution. We therefore seek the bounded-singular solution of the tangential boundary value problem defined by the displacements of (3(i)).

3.1. A particular solution

If a tangential force Q is applied to the surface of an elastic half plane in the direction of the positive x-axis, the resulting tangential surface displacement can be written

$$u_x = -\frac{2Q}{\pi E^*} \ln\left|\frac{x}{d}\right|, \tag{9}$$

where d is a length scale introduced to maintain dimensional consistency. The length d represents a rigid-body displacement and is strictly arbitrary in two-dimensional contact problems, since the displacement field is logarithmically unbounded at infinity, which prevents us from taking the point at infinity as a reference. However the results are only weakly dependent on the choice of the length scale d, which can therefore conveniently be associated with some measure of the finite dimensions of the contacting body such as the radius of the wheel.

Using Eq. (9) as a Green's function, it is readily verified that the traction distribution

$$\begin{aligned} q(s,\xi) &= \frac{1}{\sqrt{-\xi(\xi+s)}}, \quad -s < \xi < 0 \\ &= 0, \quad \xi > 0 \text{ and } \xi < -s \end{aligned} \tag{10}$$

corresponding to the total force

$$Q = \int_{-s}^{0} \frac{\mathrm{d}\xi}{\sqrt{-\xi(\xi+s)}} = \pi \tag{11}$$

produces the tangential displacement

$$\begin{aligned} u_x(x) &= -\frac{2}{E^*} \ln\left(\frac{s}{4d}\right), \quad -s < x < 0 \\ &= -\frac{2}{E^*} \ln\left(\frac{|2x+s|}{4d} + \sqrt{\frac{x(x+s)}{4d^2}}\right), \quad x > 0 \text{ and } x < -s. \end{aligned}$$

In particular, the displacement at the point $x = 0$ is

$$u_x(0) = -\frac{2}{E^*} \ln\left(\frac{s}{4d}\right) \tag{12}$$

and the displacement derivative is

$$\begin{aligned} \frac{\mathrm{d}u_x}{\mathrm{d}x} \equiv U(s,x) &= 0, \quad -s < x < 0 \\ &= -\frac{2\,\mathrm{sgn}(x)}{E^* \sqrt{x(x+s)}}, \quad x > 0 \text{ and } x < -s. \end{aligned} \tag{13}$$

3.2. Development of a transform solution

More general traction distributions can now be constructed by superposition in the form

$$\begin{aligned} q(\xi) = \int_0^c q(s,\xi) g(s)\,\mathrm{d}s &= \int_{-\xi}^{c} \frac{g(s)\,\mathrm{d}s}{\sqrt{-\xi(\xi+s)}}, \quad -c < \xi < 0 \\ &= 0, \quad \xi > 0 \text{ and } \xi < -c. \end{aligned} \tag{14}$$

where $g(s)$ is an arbitrary function. In effect, this is a transform solution representing a superposition of linear multipliers of the distribution $q(s,\xi)$ over a range of values of s between zero and c. Expressions for the corresponding total force and tangential displacements are obtained by the same superposition using Eqs. (11)–(13) and are

$$Q = \pi \int_0^c g(s)\,\mathrm{d}s, \tag{15}$$

$$u_x(0) = -\frac{2}{E^*} \int_0^c \ln\left(\frac{s}{4d}\right) g(s)\,\mathrm{d}s, \tag{16}$$

$$\frac{\mathrm{d}u_x}{\mathrm{d}x} = \int_0^c U(s,x) g(s)\,\mathrm{d}s = \frac{2}{E^*} \int_0^{-x} \frac{g(s)\,\mathrm{d}s}{\sqrt{x(x+s)}}, \quad -c < x < 0. \tag{17}$$

If $g(s)$ is a bounded function in $0 < s < c$, Eq. (14) defines a general traction distribution in $-c < \xi < 0$ that is square-root singular at $\xi = 0$ and square-root bounded at $\xi = c$. In particular, we can define the stress intensity factor K_{II} at $\xi = 0$ as

$$K_{\mathrm{II}} \equiv \lim_{\xi \to 0^+} q(\xi) \sqrt{-2\pi\xi} = \sqrt{2\pi} \int_0^c \frac{g(s)\,\mathrm{d}s}{\sqrt{s}}. \tag{18}$$

3.3. Inversion of the transform

Suppose that $\mathrm{d}u_x/\mathrm{d}x$ in Eq. (17) is a known function $h(x)$ in $-c < x < 0$ and we wish to find the corresponding value of $g(s)$. We then have

$$\frac{2}{E^*} \int_0^{-x} \frac{g(s)\,\mathrm{d}s}{\sqrt{x(x+s)}} = h(x), \quad -c < x < 0$$

which defines an Abel integral equation whose solution is

$$g(s) = \frac{E^*}{2\pi} \frac{\mathrm{d}}{\mathrm{d}s} \int_0^s \frac{h(-z)\sqrt{z}\,\mathrm{d}z}{\sqrt{s-z}}. \tag{19}$$

Substituting this result into Eq. (15), we obtain

$$Q = \pi \int_0^b g(s)\,\mathrm{d}s = \frac{E^*}{2} \int_0^s \frac{h(-z)\sqrt{z}\,\mathrm{d}z}{\sqrt{s-z}}\bigg|_{s=0}^{s=c} = \frac{E^*}{2} \int_0^c \frac{h(-z)\sqrt{z}\,\mathrm{d}z}{\sqrt{c-z}} \tag{20}$$

Similarly, substituting Eq. (19) into Eqs. (16) and (18) and simplifying the resulting expressions, we obtain

$$u_x(0) = -\frac{1}{\pi}\ln\left(\frac{c}{4d}\right)\int_0^c \frac{h(-z)\sqrt{z}\,\mathrm{d}z}{\sqrt{c-z}} + \frac{2}{\pi}\int_0^c h(-z)\arctan\left(\sqrt{\frac{c}{z}-1}\right)\mathrm{d}z, \tag{21}$$

$$K_{\mathrm{II}} = \frac{E^*}{\sqrt{2\pi c}}\int_0^c \left(\sqrt{\frac{z}{c-z}} + \sqrt{\frac{c-z}{z}}\right)h(-z)\,\mathrm{d}z. \tag{22}$$

The mathematical operations involved in developing these expressions are given in Appendix A.

3.4. Time invariant terms

The time-invariant term $u(x) = u_0(x)$ in the displacement corresponds to

$$h_0(x) = \frac{\mathrm{d}u_x}{\mathrm{d}x} = \frac{\mathrm{d}u_0}{\mathrm{d}x} = 1 - \frac{\Omega_0 R}{V} \equiv \varepsilon \tag{23}$$

from (4(i)), where ε is the mean creep ratio. Substituting into Eq. (20) and evaluating the resulting integral, we obtain

$$Q = \frac{E^*\varepsilon}{2}\int_0^c \frac{\sqrt{z}\,\mathrm{d}z}{\sqrt{c-z}} = \frac{E^*\varepsilon\pi c}{4} = \frac{E^*\varepsilon\pi a}{2} \tag{24}$$

since the total contact length is $c = 2a$. Also, from Eq. (22) we obtain the time-invariant term in the stress intensity factor as

$$K_{\mathrm{II}} = \frac{E^*\varepsilon}{\sqrt{2\pi c}}\int_0^c \left(\sqrt{\frac{z}{c-z}} + \sqrt{\frac{c-z}{z}}\right)\mathrm{d}z = E^*\varepsilon\sqrt{\frac{\pi c}{2}} = E^*\varepsilon\sqrt{\pi a}. \tag{25}$$

These results agree of course with the classical steady-state solution of Carter [2].

3.5. Oscillating terms

The oscillating term $u_1(x)$ in Eq. (4(ii)) contributes an additional term

$$h_1(z) = \frac{\partial}{\partial x}u_1(x)\exp(\imath\omega t)\Big|_{x=z+a} = -\frac{\imath\omega C_1}{V}\exp\left(-\frac{\imath\omega(z+a)}{V}\right)\exp(\imath\omega t), \tag{26}$$

where we are measuring x from the mid-point of the contact in defining $u(x)$, so the trailing edge $x = a$ corresponds to $z = 0$.

Substituting this expression into Eq. (20), we obtain the contribution to Q from the time-varying term $u_1(x)$ as

$$Q = -\frac{\imath\omega C_1 E^*}{2V}\exp(\imath\omega t)\exp\left(-\frac{\imath\omega a}{V}\right)\int_0^{2a}\exp\left(\frac{\imath\omega z}{V}\right)\frac{\sqrt{z}\,\mathrm{d}z}{\sqrt{2a-z}}$$

and using the substitution $z = a(1+s)$,

$$Q = -\frac{\imath E^* a\omega C_1}{2V}I_1\left(\frac{\omega a}{V}\right)\exp(\imath\omega t), \tag{27}$$

where

$$I_1(p) = \int_{-1}^{1}\exp(\imath ps)\sqrt{\frac{1+s}{1-s}}\,\mathrm{d}s = \pi\{J_0(p) + \imath J_1(p)\} \tag{28}$$

as shown in Appendix B, where J_0, J_1 are Bessel functions of the first kind. For the stress intensity factor, we substitute Eq. (26) into Eq. (22) obtaining

$$K_{\mathrm{II}} = -\frac{\imath\omega C_1 E^*}{V\sqrt{4\pi a}}\exp\left(-\frac{\imath\omega a}{V}\right)\exp(\imath\omega t) \times \int_0^{2a}\left(\sqrt{\frac{z}{2a-z}} + \sqrt{\frac{2a-z}{z}}\right)\exp\left(\frac{\imath\omega z}{V}\right)\mathrm{d}z$$

and using the substitution $z = a(1+s)$,

$$K_{\mathrm{II}} = -\frac{\imath\omega C_1 E^*}{V}\sqrt{\frac{a}{4\pi}}\left[I_1\left(\frac{\omega a}{V}\right) + I_2\left(\frac{\omega a}{V}\right)\right]\exp(\imath\omega t), \tag{29}$$

where

$$I_2(p) = \int_{-1}^{1}\exp(\imath ps)\sqrt{\frac{1-s}{1+s}}\,\mathrm{d}s = \pi\{J_0(p) - \imath J_1(p)\} \tag{30}$$

as shown in Appendix B.

3.6. Perturbations in Q and K_{II}

We assume that the sinusoidal perturbation is sufficiently small for the analysis to be linear and hence the tangential force Q and the stress intensity factor K_{II} can be obtained by superposing the contributions from the time-invariant and oscillating terms. For Q, we obtain

$$Q = \frac{E^*\varepsilon\pi a}{2} - \frac{\imath E^* a\omega C_1}{2V}I_1\left(\frac{\omega a}{V}\right)\exp(\imath\omega t)$$

from Eqs. (24) and (27). Substituting for $a(t)$ from Eq. (7) and dropping second order terms in the perturbation, we obtain

$$Q_0 = \frac{E^*\varepsilon\pi a_0}{2}, \quad Q_1 = \frac{E^*\varepsilon\pi a_1}{2} - \frac{\imath E^* a_0\omega C_1}{2V}I_1\left(\frac{\omega a_0}{V}\right) \tag{31}$$

for the coefficients in (5(ii)).

For the stress intensity factor, we have

$$K_{\mathrm{II}} = E^*\varepsilon\sqrt{\pi a} - \frac{\imath\omega C_1 E^*\sqrt{\pi a}}{V}J_0\left(\frac{\omega a}{V}\right)\exp(\imath\omega t)$$

from Eqs. (25), (28)–(30). Substituting for $a(t)$ from Eq. (7), performing a linear perturbation about a_0 and retaining only the first order terms, we obtain

$$K_{\mathrm{II}} = K_0 + K_1\exp(\imath\omega t), \tag{32}$$

where

$$K_0 = E^*\varepsilon\sqrt{\pi a_0}, \quad K_1 = \frac{E^*\varepsilon a_1}{2}\sqrt{\frac{\pi}{a_0}} - \frac{\imath\omega C_1 E^*\sqrt{\pi a_0}}{V}J_0\left(\frac{\omega a_0}{V}\right). \tag{33}$$

3.7. Determining the constant C_1

To complete the solution, we need to determine the constant C_1 in terms of the perturbations Ω_1, a_1 in rotational speed and contact semi-width. To do this, we shall use Eq. (21) to determine the displacement at the instantaneous trailing edge of the contact. Equating this to $u_x(a)$ and equating the first order perturbation terms will yield an equation for C_1.

For the time-invariant term $h_0(x)$, we have

$$u_x(0) = -\frac{\varepsilon}{\pi}\ln\left(\frac{a}{2d}\right)\int_0^{2a}\frac{\sqrt{z}\,\mathrm{d}z}{\sqrt{2a-z}} + \frac{2\varepsilon}{\pi}\int_0^{2a}\arctan\left(\sqrt{\frac{2a}{z}-1}\right)\mathrm{d}z = \varepsilon a\left[1 - \ln\left(\frac{a}{2d}\right)\right] \tag{34}$$

from Eqs. (21) and (23).

For the oscillating term $h_1(x)$ of Eq. (26),

$$u_x(0) = \frac{\imath\omega C_1}{\pi V}\exp\left(-\frac{\imath\omega a}{V}\right)\exp(\imath\omega t)\left[\ln\left(\frac{a}{2d}\right)\int_0^{2a}\exp\left(\frac{\imath\omega z}{V}\right)\frac{\sqrt{z}\,\mathrm{d}z}{\sqrt{2a-z}} - 2\int_0^{2a}\exp\left(\frac{\imath\omega z}{V}\right)\arctan\left(\sqrt{\frac{2a}{z}-1}\right)\mathrm{d}z\right].$$

With the substitution $z = a(1+s)$,

$$u_x(0) = \frac{\imath\omega C_1 a}{\pi V}\exp(\imath\omega t)\left[\ln\left(\frac{a}{2d}\right)I_1\left(\frac{\omega a}{V}\right) - 2I_3\left(\frac{\omega a}{V}\right)\right], \tag{35}$$

where

$$I_3(p)=\int_{-1}^{1}\mathrm{e}^{\imath ps}\arctan\left(\sqrt{\frac{1-s}{1+s}}\right)\mathrm{d}s=\frac{\imath\pi}{2p}(\mathrm{e}^{-\imath p}-J_0(p)) \tag{36}$$

as shown in Appendix B.

The sum of Eqs. (34) and (35) defines the tangential displacement at the trailing edge $x=a$. Using Eqs. (3) and (4), we therefore have

$$\varepsilon a\left[1-\frac{1}{2}\ln\left(\frac{a}{2d}\right)\right]+\frac{\imath\omega C_1 a}{\pi V}\exp(\imath\omega t)\left[\ln\left(\frac{a}{2d}\right)I_1\left(\frac{\omega a}{V}\right)-2I_3\left(\frac{\omega a}{V}\right)\right]$$
$$=\varepsilon a+C_0+\left[\frac{\imath\Omega_1 R}{\omega}+C_1\exp\left(-\frac{\imath\omega a}{V}\right)\right]\exp(\imath\omega t).$$

Substituting for a from Eq. (7), performing a linear perturbation about a_0 retaining only the first order terms and separating time-invariant and oscillating terms, we obtain

$$C_0=-\varepsilon a_0\ln\left(\frac{a_0}{2d}\right)$$

$$C_1=-\left[\varepsilon a_1\left\{\ln\left(\frac{a_0}{2d}\right)+1\right\}+\frac{\imath\Omega_1 R}{\omega}\right]$$
$$\Big/\left[J_0\left(\frac{\omega a_0}{V}\right)-\frac{\imath\omega a_0}{\pi V}I_1\left(\frac{\omega a_0}{V}\right)\ln\left(\frac{a_0}{2d}\right)\right], \tag{37}$$

where we have used Eq. (36) to simplify the expression for C_1.

3.8. Receptances

The final step is to use Eqs. (37), (8)(ii), (31)(i) to eliminate C_1, a_1, ε, respectively, in Eq. (31)(ii), giving

$$Q_1=Q_P(\zeta)P_1+Q_\Omega(\zeta)\Omega_1,$$

where

$$Q_P=\frac{Q_0}{2P_0}\left[1+\frac{\imath\zeta}{2\pi D(\zeta)}\left\{\ln\left(\frac{a_0}{2d}\right)+1\right\}I_1\left(\frac{\zeta}{2}\right)\right],$$
$$Q_\Omega=-\frac{E^*Ra_0}{2VD(\zeta)}I_1\left(\frac{\zeta}{2}\right),$$

$$D(\zeta)=J_0\left(\frac{\zeta}{2}\right)-\frac{\imath\zeta}{2\pi}I_1\left(\frac{\zeta}{2}\right)\ln\left(\frac{a_0}{2d}\right) \tag{38}$$

and ζ is defined in Eq. (1).

3.9. Energy dissipation

For finite coefficients of friction, a slip zone is generated adjacent to the trailing edge of the contact area. As the coefficient of friction is allowed to grow without limit, the corresponding energy dissipation rate W tends to a finite limit which is the energy release rate associated with the moving singular traction field—i.e.

$$W=\frac{VK_{\mathrm{II}}^2}{2E^*}.$$

Using Eq. (32) for K_{II} and dropping the second order terms. we obtain

$$W=W_0+W_1\exp(\imath\omega t)$$

with

$$W_0=\frac{VK_0^2}{2E^*},\quad W_1=\frac{VK_0K_1}{E^*}. \tag{39}$$

To obtain K_0, K_1, we use Eqs. (37), (8)(ii), (31)(i) to eliminate C_1, a_1, ε, respectively, in Eq. (33), giving

$$K_0=\frac{2Q_0}{\sqrt{\pi a_0}},\quad K_1=K_P(\zeta)P_1+K_\Omega(\zeta)\Omega_1,$$

where

$$K_P=\frac{Q_0}{2P_0\sqrt{\pi a_0}}\left[1+\frac{\imath\zeta}{D(\zeta)}J_0\left(\frac{\zeta}{2}\right)\left\{\ln\left(\frac{a_0}{2d}\right)+1\right\}\right],$$
$$K_\Omega=-\frac{E^*R\sqrt{\pi a_0}}{VD(\zeta)}J_0\left(\frac{\zeta}{2}\right).$$

Using these results in Eq. (39), we then have

$$W_0=\frac{2VQ_0^2}{\pi E^* a_0},\quad W_1=W_P(\zeta)P_1+W_\Omega(\zeta)\Omega_1,$$

where

$$W_P=\frac{Q_0^2V}{\pi a_0E^*P_0}\left[1+\frac{\imath\zeta}{D(\zeta)}J_0\left(\frac{\zeta}{2}\right)\left\{\ln\left(\frac{a_0}{2d}\right)+1\right\}\right],$$
$$W_\Omega=-\frac{2Q_0R}{D(\zeta)}J_0\left(\frac{\zeta}{2}\right). \tag{40}$$

3.10. The limiting case $\zeta\to 0$

In the limit where $\zeta\to 0$, the expressions (38) and (40) for Q_P, Q_Ω, W_P, W_Ω reduce to

$$Q_P(0)=\frac{Q_0}{2P_0},\quad Q_\Omega(0)=-\frac{\pi E^*Ra_0}{2V},$$
$$W_P=\frac{VQ_0^2}{a_0P_0\pi E^*},\quad W_\Omega(0)=-2RQ_0. \tag{41}$$

These are also the expressions that are obtained if it is assumed that the solution for steady rolling due to Carter [2] also applies under transient conditions. This is reasonable since $\zeta\to 0$ corresponds to the case where the oscillation is extremely slow relative to the translational velocity V.

3.11. Choice of the parameter d

As explained in Section 3.1, the parameter d is strictly arbitrary for two-dimensional problems for the half plane, and it is clear from Eqs. (38) and (40) that the value will affect the corresponding receptances, albeit fairly weakly since the logarithm is a slowly varying function.

If the problem is strictly two-dimensional, as in the case of two elastic cylinders rolling together under plane strain conditions, we would expect the appropriate value of d to be comparable with the radius R of the cylinders. The related problem of the compression of a circular cylinder between two contacting bodies was discussed by Johnson [3, Section 5.6], who finds that the rigid body compression using an exact two-dimensional formulation differs from that using the half-plane approximation by only 10% if d is taken to be equal to R.

The two-dimensional analysis can also be used as an approximation for the three-dimensional case where the contact region is much longer in the transverse direction (parallel with the wheel axle) than in the direction of motion. Kalker [12] used the matched asymptotic expansion method to expand the general three-dimensional deformation in powers of the small parameter defining the ratio between the small and large dimensions of the contact region. The first term in this expansion is a two-dimensional solution, but the logarithmic term, corresponding here to the choice of d, is contained in the second term which for more general problems can be obtained as the solution of a line integral equation with a logarithmic kernel. In particular, the tangential compliance of an elliptical contact of semi-axes a, b will be equal to that of a two-dimensional contact of semi-width a with the same force per unit width if the latter is determined using the value $d=2b$. Kalker showed that the matched

asymptotic expansion gave acceptable results even for values of b/a as low as 2.

4. Results

In this section, we shall explore the effect of ζ on the receptances as defined by Eqs. (38) and (40) for values of d appropriate to two-dimensional or narrow elliptical contacts. We shall also compare the results with previously published predictions based on the Winkler approximation [11] which can be summarized in the present notation as

$$Q_P = \frac{2a_0 k_q Q_0}{P_0 \pi E^*}\left[1 - \frac{\imath}{\zeta}[1 - \exp(-\imath\zeta)]\right],$$
$$Q_\Omega = -\frac{4a_0^2 k_q R}{V\zeta}\left[\frac{1}{\zeta}[1 - \exp(-\imath\zeta)] - \imath\right],$$
$$W_P = \frac{4k_q V Q_0^2}{P_0 \pi^2 E^{*2}}[1 + \exp(-\imath\zeta)],$$
$$W_\Omega = \frac{8\imath R Q_0 a_0 k_q}{\pi E^*}\frac{[1 - \exp(-\imath\zeta)]}{\zeta}, \quad (42)$$

where k_q is the Winkler modulus for tangential loading (such that the tangential traction is related to the local tangential elastic displacement through $q(x) = k_q u_x(x)$). This modulus is a free parameter that can be chosen to fit an appropriate continuum solution, such as the Carter solution (41) in the limit $\zeta \to 0$. However, since there is only one free parameter, it proves possible to choose k_q so as to match the either receptances $Q_P(0), W_P(0)$ or $Q_\Omega(0), W_\Omega(0)$, but not all four. Ciavarella and Barber [11] chose the latter option, in which case the Winkler solution then overestimates $Q_P(0), W_P(0)$ in this limit by a factor of 2.

An alternative approach which is difficult to justify from a mechanics perspective, but which makes more sense if the Winkler solution is seen as a curve-fitting model is to use different values of k_q in the two pairs of expressions, so as to ensure that all four are correct at $\zeta = 0$. In this context, it is worth remarking that in a corrugation calculation, the most important factor is the relative phase of the excitation and the resulting wear, since those wavelengths grow for which the maximum wear occurs at the troughs of the original corrugation. All four receptances are real and positive at $\zeta = 0$, so renormalization of two of the receptances has no effect on the phase plot.

Ciavarella and Barber [11] used the Winkler receptances (42) in an idealized rail-wheel dynamic model to predict the wavelength of corrugations to be expected as a function of vehicle speed V. Since the receptances are defined by closed-form expressions, it is then possible to explore the expected behaviour in some detail. In particular, the preferred corrugation wavelength is expected to be that with the highest growth rate at the troughs of the exciting corrugation—i.e. the largest negative real part in the dissipation function. The results showed remarkably good agreement with a range of previously published experimental data.

Fig. 2 shows the receptance Q_Ω defined by Eq. (38) and normalized by $Q_\Omega(0)$ from Eq. (41). Fig. 2(a) is a Nyquist (polar)

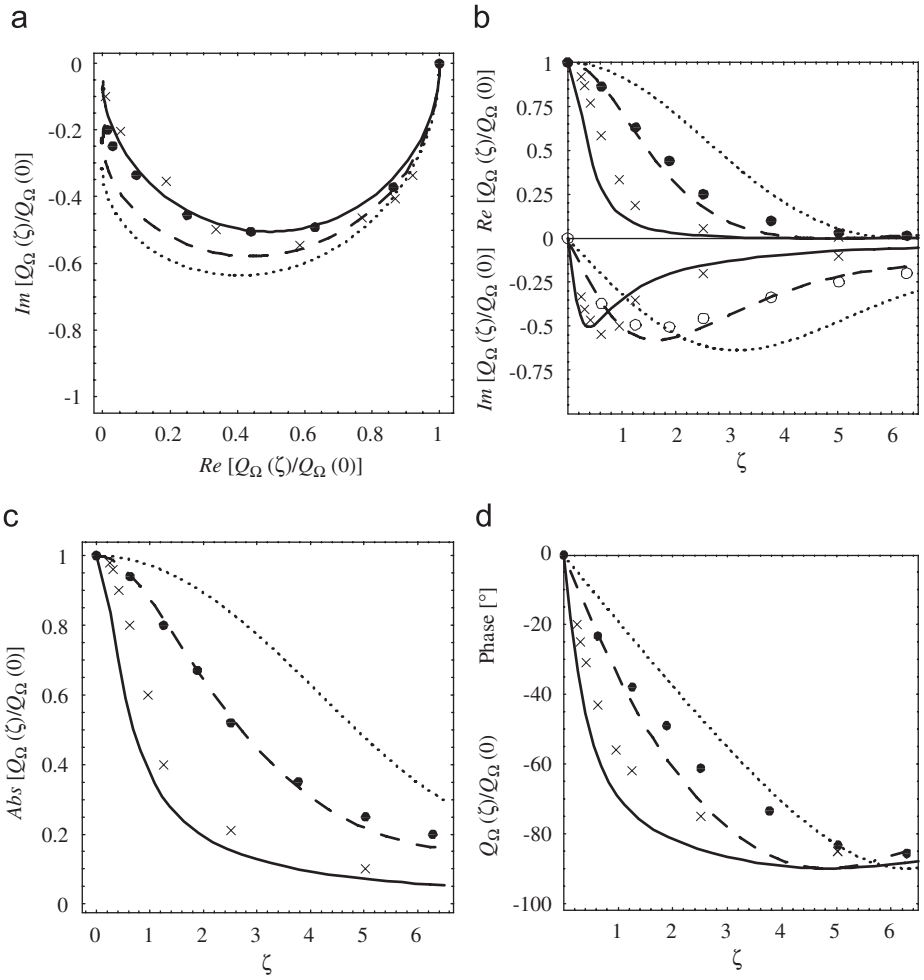

Fig. 2. The receptance $Q_\Omega(\zeta)/Q_\Omega(0)$. ——— the two-dimensional solution; — — — elliptical approximation for $b/a_0 = 1.5$; ····· Winkler approximation; ••• Three-dimensional predictions from Gross-Thebing.

plot, Fig. 2(b) presents the real and imaginary parts as a function of ζ and Fig. 2(c) and Fig. 2(d) present the magnitude and phase also as functions of ζ. The solid line corresponds to the case $d = 125a_0$, which is representative of the two-dimensional solution with $d = R$—e.g. for a wheel of radius $R = 500$ mm, with $a_0 = 4$ mm. The dashed line represents the same expressions using $d = 3a_0$ which is appropriate for Kalker's line contact theory with a ratio of semi-axes $b/a_0 = 1.5$. This is about as low an ellipticity as can reasonably be treated by this approach and hence the two lines bracket the effective range covered by possible variation of the parameter d. The dotted line represents the Winkler solution of Eq. (42(ii)), normalized to its value at $\zeta = 0$.

The circles in Fig. 2 represent values from the three-dimensional analysis of Gross-Thebing [13,14] for an elliptical contact with semi-axes $a_0 = 4.8$ mm, $b = 7.2$ mm and hence $b/a_0 = 1.5$. Gross-Thebing obtained these results by using Kalker's CONTACT code [9] to solve the transient frictional contact problem under a range of conditions and then performing a perturbation analysis on the numerical results. More details of this calculation procedure are given by Knothe [15]. The code uses a variational formulation of the continuum elastic contact problem and hence provides an accurate but extremely computer-intensive solution of the perturbation problem. Also, the large number of parameters involved imposes limits on the practicality of archiving a full range of numerical data. However, a comparison of the Gross-Thebing results with the dashed line in Fig. 2 (which is the appropriate result for $b/a_0 = 1.5$) shows remarkably good agreement in view of the idealizations involved. Notice also that for corrugation wavelengths of 40 mm or more, values of ζ will not be much greater than unity and in this range the agreement with Gross-Thebing's results is even better. The crosses in Fig. 2 represent data for a more elliptical contact $b/a_0 = 10$, using data taken from Alonso and Giménez [16] who also used Gross-Thebing's method. As we should expect, the results are closer to the two-dimensional curve (solid line). Even better agreement was obtained with the present closed-form expressions using $d = 2b = 20a_0$, but this line is omitted in the interests of clarity.

Figs. 3–5 show corresponding plots of the remaining normalized receptances Q_P, W_Ω, W_P, respectively, from Eqs. (38), (40), (42) using the same parameter values and line styles. We notice from Fig. 4(c) that W_Ω passes through zero at $\zeta = 4.81$ implying that there will be no dissipation associated with oscillations in rotational speed at this frequency. In fact, W_Ω passes through zero at each of the zeros of the Bessel function $J_0(\zeta/2)$. This special case was already identified by Kalker [4].

All the receptances except W_P decay with increasing ζ and lie predominantly below the real line in the Nyquist plot implying phase lags of less than 90°. However, the dissipation coefficient W_P makes a complete circle in the Nyquist plot, showing that the receptance as $\zeta \to \infty$ is the same as that at zero. The two-dimensional solution ($d = 120a_0$) exhibits a range in which the real part is negative implying that the dissipation and hence wear at the point of minimum normal force exceeds that at maximum normal force. By contrast, that for $d = 3a_0$ passes close to zero, implying a value of ζ at which dissipation is minimal.

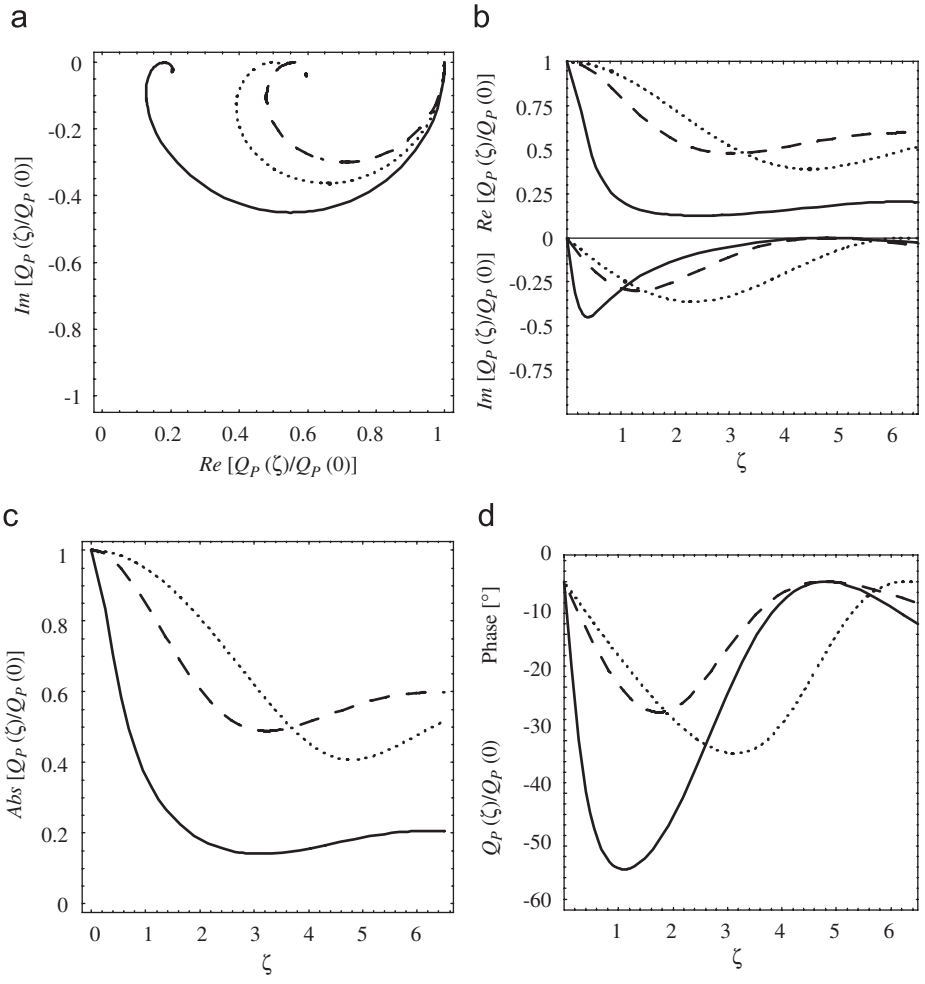

Fig. 3. The receptance $Q_P(\zeta)/Q_P(0)$. ——— the two-dimensional solution; — — — elliptical approximation for $b/a_0 = 2$; · · · · · · · · · Winkler approximation.

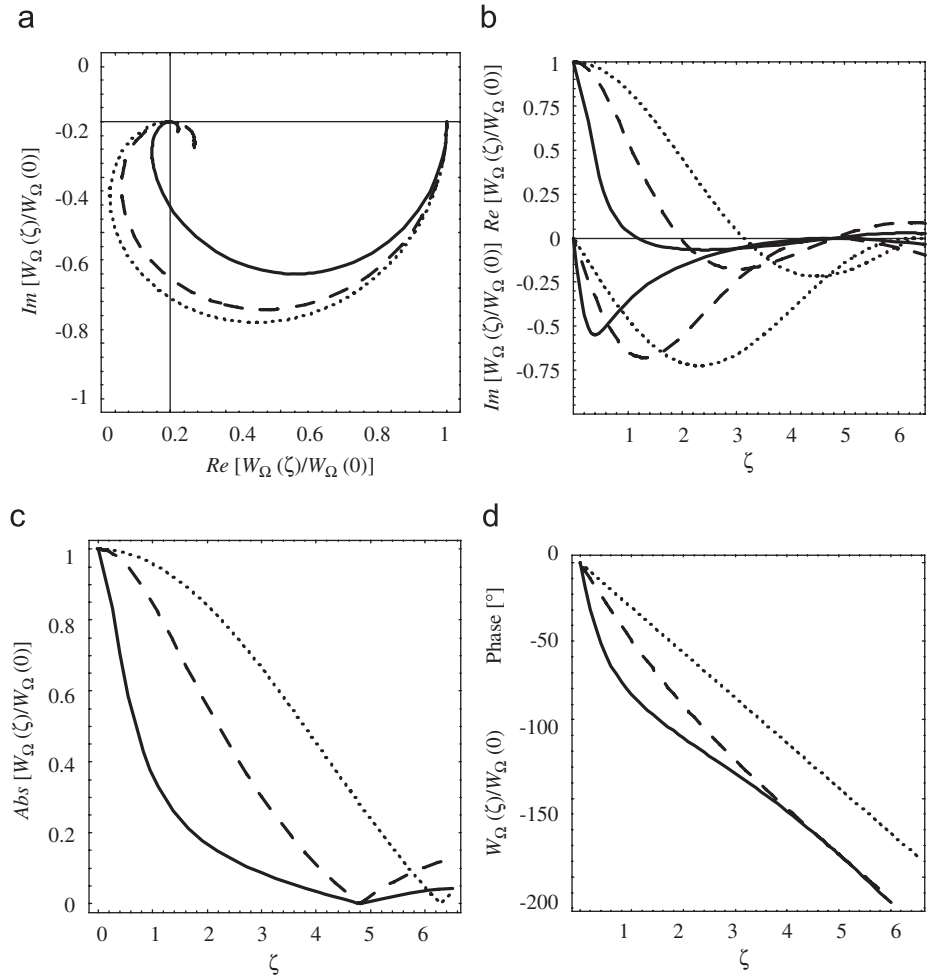

Fig. 4. The receptance $W_\Omega(\zeta)/W_\Omega(0)$. —— the two-dimensional solution; — — — elliptical approximation for $b/a_0 = 2$; ····· Winkler approximation.

Gross-Thebing's model is for a three-dimensional elliptical contact and hence the coefficients he reports for variation in normal force P include influences both from consequent variation of a_0 and b. It is therefore not possible to make a direct comparison with the present results for Q_P, since changes in b would also imply changes in the appropriate value of the parameter d. Also, though Gross-Thebing writes the energy dissipation as an integral over the slip region, he does not provide expressions for the dissipation coefficients that are directly comparable to our W_Ω, W_P. However, the excellent agreement observed in Fig. 2 suggests that the results for the remaining coefficients can be used confidently for elliptical contact.

Figs. 2–5 show that the Winkler approximation of Eqs. (42) exhibits the same functional form as the exact continuum equivalents, but consistently underestimates the rate at which the receptance is modified with increasing ζ. For example, all the results in Fig. 2(b) show $\Im(Q_\Omega)$ reaching a minimum of about $-0.6Q_\Omega(0)$, but the Winkler curve reaches this minimum at a larger value of ζ. Kalker's FASTSIM algorithm is based on what is essentially a Winkler solution of the contact problem and we should therefore anticipate a similar underestimate in the many contact models using this algorithm. This can be seen for example in Figs. 2 and 3 of [16].

5. Conclusions

We have developed closed-form expressions for the receptances of a tractive elastic rolling cylinder subjected to sinusoidal oscillations in normal force and rotational speed in the limit of high coefficient of friction. We also present results for the rate of energy dissipation, which is generally considered to correlate with the wear rate. The results can also be applied to three-dimensional rolling contact problems involving an elliptical contact area, provided that the ellipse is sufficiently elongated in the direction of the rotation axis. The resulting receptances show very good correlation with numerical results obtained by Gross-Thebing, using a computer-intensive variational solution of the elastic contact problem. Being in closed form, they therefore provide a useful resource for investigations of corrugations in railway tracks. Comparison was also made with a 'Winkler' solution of the same problem—a simplification that is widely used in corrugation studies (often in the context of Kalker's FASTSIM algorithm) because it significantly reduces the extent of the required computations. The comparison shows that a Winkler approximation exhibits the correct functional form for the receptance in all cases, but underestimates the rate at which the receptance is modified by decreasing wavelength, so that the error becomes most significant at short wavelengths.

Appendix A

Substituting Eq. (19) into Eq. (16) and integrating by parts, we have

$$u_x(0) = -\frac{1}{\pi}\left[\int_0^s \frac{h(-z)\sqrt{z}\,\mathrm{d}z}{\sqrt{s-z}}\ln\left(\frac{s}{4d}\right)\right]_{s=0}^{s=c} + \frac{1}{\pi}\int_0^c\left(\int_0^s \frac{h(-z)\sqrt{z}\,\mathrm{d}z}{\sqrt{s-z}}\right)\frac{\mathrm{d}s}{s}. \tag{43}$$

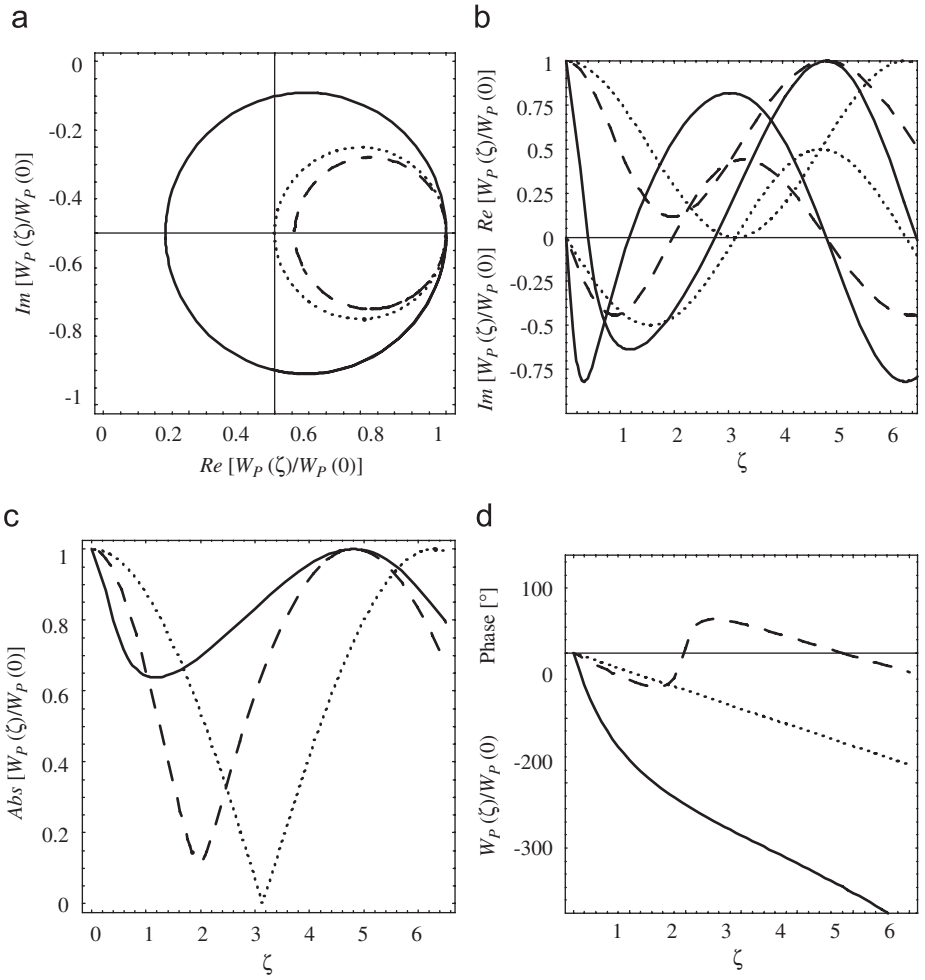

Fig. 5. The receptance $W_P(\zeta)/W_P(0)$. —— the two-dimensional solution; — — — elliptical approximation for $b/a_0 = 2$; ····· Winkler approximation.

Reversing the order of integration in the second term, we have

$$\frac{1}{\pi}\int_0^c\left(\int_0^s \frac{h(-z)\sqrt{z}\,\mathrm{d}z}{\sqrt{s-z}}\right)\frac{\mathrm{d}s}{s} = \frac{1}{\pi}\int_0^c h(-z)\sqrt{z}\left(\int_z^c \frac{\mathrm{d}s}{s\sqrt{s-z}}\right)\mathrm{d}z. \quad (44)$$

Using the substitution $s = z(p^2+1)$, the inner integral can be evaluated as

$$\int_z^c \frac{\mathrm{d}s}{s\sqrt{s-z}} = \frac{2}{\sqrt{z}}\int_0^{\sqrt{(c-z)/z}} \frac{\mathrm{d}p}{p^2+1} = \frac{2}{\sqrt{z}}\arctan\left(\sqrt{\frac{c}{z}-1}\right)$$

and using this result in Eqs. (44) and (43),

$$u_x(0) = -\frac{1}{\pi}\ln\left(\frac{c}{4d}\right)\int_0^c \frac{h(-z)\sqrt{z}\,\mathrm{d}z}{\sqrt{c-z}} + \frac{2}{\pi}\int_0^c h(-z)\arctan\left(\sqrt{\frac{c}{z}-1}\right)\mathrm{d}z.$$

Next, substituting Eq. (19) into Eq. (18) and integrating by parts, we have

$$K_{\mathrm{II}} = \frac{E^*}{\sqrt{2\pi}}\left[\frac{1}{\sqrt{s}}\int_0^s \frac{h(-z)\sqrt{z}\,\mathrm{d}z}{\sqrt{s-z}}\right]_{s=0}^{s=c} + \frac{E^*}{2\sqrt{2\pi}}\int_0^c\left(\int_0^s \frac{h(-z)\sqrt{z}\,\mathrm{d}z}{\sqrt{s-z}}\right)\frac{\mathrm{d}s}{s^{3/2}}. \quad (45)$$

Reversing the order of integration in the second term,

$$\int_0^c\left(\int_0^s \frac{h(-z)\sqrt{z}\,\mathrm{d}z}{\sqrt{s-z}}\right)\frac{\mathrm{d}s}{s^{3/2}} = \int_0^c h(-z)\sqrt{z}\left(\int_z^c \frac{\mathrm{d}s}{s^{3/2}\sqrt{s-z}}\right)\mathrm{d}z. \quad (46)$$

Using the substitution $s = z(p^2+1)$, the inner integral can be evaluated as

$$\int_z^c \frac{\mathrm{d}s}{s^{3/2}\sqrt{s-z}} = \frac{2}{z}\int_0^{\sqrt{(c-z)/z}} \frac{\mathrm{d}p}{(p^2+1)^{3/2}} = \frac{2}{z}\sqrt{1-\frac{z}{c}}$$

and hence, using Eqs. (46) and (45),

$$K_{\mathrm{II}} = \frac{E^*}{\sqrt{2\pi c}}\int_0^c \frac{h(-z)\sqrt{z}\,\mathrm{d}z}{\sqrt{c-z}} + \frac{E^*}{\sqrt{2\pi c}}\int_0^c\left(\sqrt{\frac{c-z}{z}}\right)h(-z)\mathrm{d}z.$$

Appendix B

The complex conjugate of GR 3.384.1 [17] gives

$$\int_{-1}^1 (1-x)^{\nu-1}(1+x)^{\mu-1}\mathrm{e}^{\imath px}\,\mathrm{d}x = 2^{\mu+\nu-1}B(\mu,\nu)\mathrm{e}^{-\imath p}{}_1F_1(\mu,\nu+\mu;2\imath p), \quad (47)$$

where ${}_1F_1$ is the degenerate hypergeometric function and $\Re(\nu)>0$, $\Re(\mu)>0$. Setting $\nu = \frac{1}{2}$, $\mu = \frac{3}{2}$,

$$I_1(p) = \int_{-1}^1 \mathrm{e}^{\imath ps}\sqrt{\frac{1+s}{1-s}}\mathrm{d}s = 2B\left(\frac{3}{2},\frac{1}{2}\right)\mathrm{e}^{-\imath p}{}_1F_1\left(\frac{3}{2},2;2\imath p\right).$$

From GR 9.213 and 8.384.1 [17] we have

$${}_1F_1\left(\frac{3}{2},2;x\right) = 2\frac{\mathrm{d}}{\mathrm{d}x}{}_1F_1\left(\frac{1}{2},1;x\right), \quad B\left(\frac{3}{2},\frac{1}{2}\right) = \frac{\Gamma(3/2)\Gamma(1/2)}{\Gamma(2)} = \frac{\pi}{2}.$$

Also, from Ref. [18, p. 191], we have

$$e^{\imath z}J_\nu(z)=\frac{(z/2)^\nu}{\Gamma(\nu+1)}{}_1F_1\left(\nu+\frac{1}{2},2\nu+1;2\imath z\right). \tag{48}$$

Combining these results, we obtain

$$I_1(p)=\frac{\pi e^{-\imath p}}{\imath}\frac{d}{dp}[e^{\imath p}J_0(p)]=\pi\{J_0(p)+\imath J_1(p)\}.$$

Using Eq. (47) with $\nu=\frac{3}{2}$, $\mu=\frac{1}{2}$, we obtain

$$I_2(p)=\int_{-1}^{1}e^{\imath ps}\sqrt{\frac{1-s}{1+s}}ds=2B\left(\frac{1}{2},\frac{3}{2}\right)e^{\imath p}{}_1F_1\left(\frac{1}{2},2;2\imath p\right).$$

Also, GR 9.212.1 gives

$${}_1F_1\left(\frac{3}{2},2;-2\imath p\right)=e^{-2\imath p}{}_1F_1\left(\frac{1}{2},2;2\imath p\right)$$

and hence

$$I_2(p)=\pi e^{\imath p}{}_1F_1\left(\frac{3}{2},2;-2\imath p\right)=I_1(-p)=\pi\{J_0(p)-\imath J_1(p)\}.$$

Integrating by parts, we have

$$I_3(p)=\int_{-1}^{1}e^{\imath ps}\arctan\left(\sqrt{\frac{1-s}{1+s}}\right)ds=-\frac{\pi e^{-\imath p}}{2\imath p}+\frac{1}{2\imath p}\int_{-1}^{1}e^{\imath ps}\frac{ds}{\sqrt{1-s^2}}$$

Using Eq. (47) with $\nu=\mu=\frac{1}{2}$, we have

$$\int_{-1}^{1}e^{\imath ps}\frac{ds}{\sqrt{1-s^2}}=B\left(\frac{1}{2},\frac{1}{2}\right)e^{-\imath p}{}_1F_1\left(\frac{1}{2},1;2\imath p\right)=\pi J_0(p)$$

using Eq. (48). Thus,

$$I_3(p)=\frac{\imath\pi}{2p}(e^{-\imath p}-J_0(p)).$$

References

[1] Archard JF. Contact and rubbing of flat surfaces. Journal of Applied Physics 1953;24:981–8.
[2] Carter FC. On the action of a locomotive driving wheel. Proceedings of the Royal Society of London Series A 1926;112:151–7.
[3] Johnson KL. Contact mechanics. Cambridge: Cambridge University Press; 1985.
[4] Kalker JJ. Transient phenomena in two elastic cylinders rolling over each other with dry friction. ASME Journal of Applied Mechanics 1970;37:677–88.
[5] Kalker JJ. A minimum principle for the law of dry friction, Part 2: application to non-steadily rolling elastic cylinders. ASME Journal of Applied Mechanics 1972;38:881–7.
[6] Mindlin RD, Deresiewicz H. Elastic spheres in contact under varying oblique forces. ASME Journal of Applied Mechanics 1953;75:327–44.
[7] Bhaskar A, Johnson KL, Wood GD, Woodhouse J. Wheel-rail dynamics with closely conformal contact, Part 1: dynamic modelling and stability analysis. Proceedings of the Institution of Mechanical Engineers, Part F 1997;211:11–26.
[8] Grassie SL, Johnson KL. Periodic microslip between a rolling wheel and a corrugated rail. Wear 1985;101:291–305.
[9] Kalker JJ. Three-dimensional elastic bodies in rolling contact. Dordrecht: Kluwer; 1990.
[10] Kalker JJ. A fast algorithm for the simplified theory of rolling contact. Vehicle System Dynamics 1982;11:1–13.
[11] Ciavarella M, Barber JR, Corrugation and the roaring rails 'enigma'. Proceedings of the Institution of Mechanical Engineers, Part J, Journal of Engineering Tribology 2008;222:171–81.
[12] Kalker JJ. On elastic line contact. ASME Journal of Applied Mechanics 1972;39:1125–32.
[13] Gross-Thebing A. Frequency-dependent creep coefficients for three dimensional rolling contact problem. Vehicle System Dynamics 1989;18:357–74.
[14] Gross-Thebing A. Lineare Modellierung des instationären Rollkontaktes von Rad und Schiene. VDI-Fortschritt-Berichte, Reihe 12, vol. 199. Düsseldorf: VDI-Verlag; 1993.
[15] Knothe K. Non-steady state rolling contact and corrugations. In: Jacobson B, Kalker JJ, editors. Rolling contact phenomena. CISM courses and lectures, vol. 411. New York: Springer Wien; 2000. p. 203–76 [chapter 4].
[16] Alonso A, Giménez JG. Non-steady state modelling of wheel-rail contact problem for the dynamic simulation of railway wheels. Vehicle System Dynamics 2007:45. 10.1080/00423110701248011.
[17] Gradshteyn IS, Ryzhik IM. Tables of integrals, series and products. New York: Academic Press; 1980.
[18] Watson GN. A treatise on the theory of Bessel functions. 2nd ed. Cambridge: Cambridge University Press; 1958.